Subwavelength far-field resolution in a square two-dimensional photonic crystal

Xiangdong Zhang
Department of Physics, Beijing Normal University, Beijing 100875, China
(Received 24 October 2004; published 16 March 2005)

It has been suggested that a subwavelength image can be realized by a photonic crystal slab with a square lattice in the lowest band. However, due to the anisotropy of dispersion in such a photonic structure, the image only appears in the near-field region. In this paper, we show that subwavelength far-field focusing and imaging, explicitly following the well-known wave-beam negative refraction law with relative refractive index of −1, can also be realized by a square photonic crystal through choosing suitable scatterers for the lowest valence band.

DOI: 10.1103/PhysRevE.71.037601 PACS number(s): 42.70.−a, 41.20.−q

Recently there has been a great deal of interest in studying an interesting class of media that have become known as left-handed materials (LHMs) [1–19]. The properties of such materials were analyzed theoretically by Veselago over 30 years ago [1], but only recently were they demonstrated experimentally [2,3]. As was shown by Vesselago, the left-handed materials possess a number of unusual electromagnetic effects [4–13]. These anomalous features allow considerable control over light propagation and open the door for a variety of applications. It is well known that an important application of negative refraction materials is the microsuperlens [1,4]. Ideally, such a superlens can focus a point source on one side of the lens into a real point image on the other side even for the case of a parallel sided slab of material. It possesses some advantages over conventional lenses. For example, it can break through the traditional limitation on lens performance and focus light onto an area smaller than a square wavelength. Recently, such image behaviors based on the LHM superlens have been observed by some numerical simulations [14–16] and experimental measurements [17–19].

It was shown that negative refraction could also occur in a photonic crystal (PC) [20–33]. The physical principles that allow negative refraction in them arise from the dispersion characteristics of wave propagation in a periodic medium, which can be described by analyzing the equifrequency surface (EFS) of the band structures [20–33]. In particular, Luo *et al.* [24] have shown that all-angle negative refraction could be achieved in the lowest band of a two-dimensional (2D) PC. The advantages of negative refraction in the lowest valence band are the single mode and high transmission. These can help us to design a microsuperlens and realize focusing of the wave. Recently, subwavelength focusing and imaging by a 2D PC slab have been observed experimentally [25–29]. However, due to the anisotropy of dispersion in a 2D PC, such images appear only in the near-field region [30–32]. Thus, extensive applications of such a phenomenon are limited. Very recently, all-angle single-beam left-handed behaviors for polarized electromagnetic (EM) waves have been demonstrated in a two-dimensional PC with a triangular lattice [33]. Good-quality non-near-field images and focusing have been observed in these systems [33,34]. In this work, we show that far-field focusing and imaging explicitly following the well-known wave-beam negative refraction law with relative refractive index of −1 can also be realized by a PC superlens with a square lattice for the lowest valence band.

We consider a 2D square lattice of coated cylinders immersed in an air background with lattice constant $a=3$ mm. The coated cylinders have metallic cores coated with a dielectric coating. The radii of metallic core and coated cylinder are $0.43a$ and $0.45a$, respectively. The dielectric constants of dielectric coating are taken as 14. For the metallic component, we use the frequency-dependent dielectric constant [35]

$$\epsilon = 1 - \frac{f_p^2}{f(f + i\gamma)}, \tag{1}$$

where f_p and γ are the plasma frequency and the absorption coefficient. Following Ref. [35], for all numerical calculations carried out in this work, we have chosen $f_p = 3600$ THz and $\gamma = 340$ THz, which corresponds to a conductivity close to that of Ti. However, our discussion and conclusions given below can apply to other metal parameters as well. We first calculate the band structure of the above system. The calculations are performed by using a highly efficient and accurate multiple-scattering Korringa-Kohn-Rostoker method [35]. The calculated results of band structure in the absence of absorption ($\gamma=0$) for the P wave are plotted in Fig. 1. We focus on the problems of wave propagation in the first band. The propagation behaviors of the EM wave in such cases can be deduced from analyzing the EFS of the band structures. The EFS contours of the above system at several relevant frequencies are demonstrated in Fig. 2.

It is clear from the figure that some low frequency contours such as 0.1 and 0.2 are very close to a perfect circle. The propagation direction of the wave is oriented to the group velocity vector which is normal to the EFS. At the lowest band, the direction of the group velocity at any point of the contour is collimated with the wave vector k, indicating that the crystal can be regarded as an effective homogeneous "right-handed" medium at these long wavelengths. However, with the increase of the frequencies, the contours

 ©2005 The American Physical Society

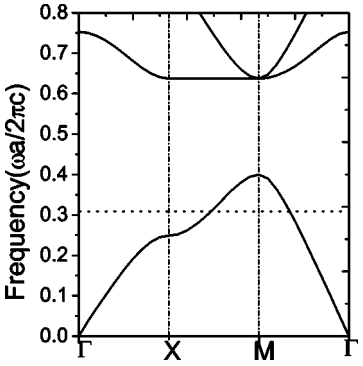

FIG. 1. The calculated photonic band structures of a square lattice of coated cylinder in air for the *P* wave. The radii of the dielectric cylinder and inner metallic cylinder are $R=0.45a$ and $r=0.43a$, respectively. The dielectric constants are $\epsilon=14$. Dotted line marks the case with relative refractive index of −1.

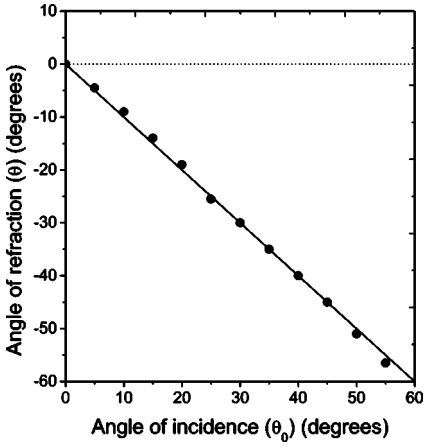

FIG. 3. The angles of refraction (θ) versus angles of incidence (θ_0) at $\omega=0.317(2\pi c/a)$. The crystal and parameters are identical to those in Fig. 1.

are significantly distorted from a circle, which are convex around point *M*. The conservation of the *k* component along the surface of refraction would result in a negative refraction effect in these cases [24–32].

In general, the convex contour around the point *M* is a square (or anisotropic) in the lowest band of a PC with a square lattice rather than a circle, as required by a homogeneous medium. Thus, when a plane wave is incident from vacuum to the PC, the refracted angles are not linearly proportional to the incident angles. This is the reason that only the near-field images have been observed in previous work [24–32]. If we can construct a circle convex around the point *M* through choosing suitable scatterers, the properties of homogeneous negative refraction materials can also be obtained in PCs according to the above analysis. The present PC system possesses such a feature. The EFS contour for $\omega=0.317(2\pi c/a)$ (marked in Fig. 2) is almost a circle around the point *M*. In the following, we investigate the relation between the incident angles and the refracted angles at this frequency by exact numerical simulation.

We take a slab sample which consists of a 20-layer coated cylinder in the air background with a square array. The surface normal of the PC slab is along the ΓM direction. The parameters of the coated cylinders are the same as the cases in Fig. 1. When a slit beam goes through the slab material, it will be refracted twice by two interfaces of the slab. There are different ray traces for the wave transmitting through the slab sample with various effective indices, when the wave is not incident on the interface in the normal direction. From the ray traces, we can deduce the effective refraction index of the slab material [32,33]. The simulations are still based on the multiple-scattering method [35]. The calculated results for the refracted angle θ versus incident angle θ_0 are summarized in Fig. 3 by the dark dots. Since the frequencies are below $0.5(2\pi c/a)$, all-angle single-beam negative refractions have been observed. More interestingly, θ is almost linearly proportional to θ_0. According to Snell's law, the effective refractive index of −1 can be obtained. This feature is close to the ideal homogeneous LHM system that can serve as a flat lens [1,4].

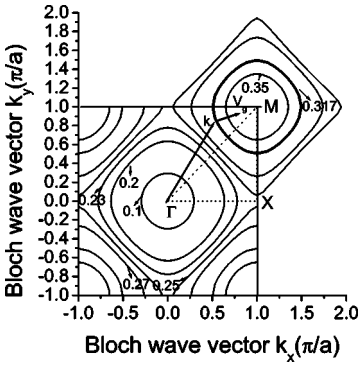

FIG. 2. Several constant-frequency contours of the first band of the 2D photonic crystal, which corresponds to the case in Fig. 1. The numbers in the figure mark the frequencies in units of $2\pi c/a$. *k* and v_g represent the wave vector and the group velocity, respectively.

In order to model such a flat lens, we take a slab sample with $40a$ width and $11a$ thickness. A continuous-wave line source is placed at a distance $5.5a$ (half thickness of the sample) from the left surface of the slab. The frequency of the incident wave emitting from such a line source is $0.317(2\pi c/a)$. If the wave transmits in such a 2D PC slab according to the well-known wave-beam negative refraction law, one should observe the focusing point in the middle of the slab and the image at the symmetric position in the opposite side of the slab, as is depicted by the simple picture on the top of Fig. 4.

To see whether or not such a phenomenon exists, we employ the multiple-scattering method [35] to calculate the propagation of waves in such a system. We adopt a real dielectric constant for metal components ($\gamma=340$ THz). In previous investigations [32,33], our calculations had shown that the position of the image does not change with the introduction of the absorption, except that the intensity of the image peak decreases. This is because the effect of the absorption on the band structure of the PC is very small [35]. Here similar phenomena are found again. A typical field intensity pattern across the above slab sample is plotted in Fig.

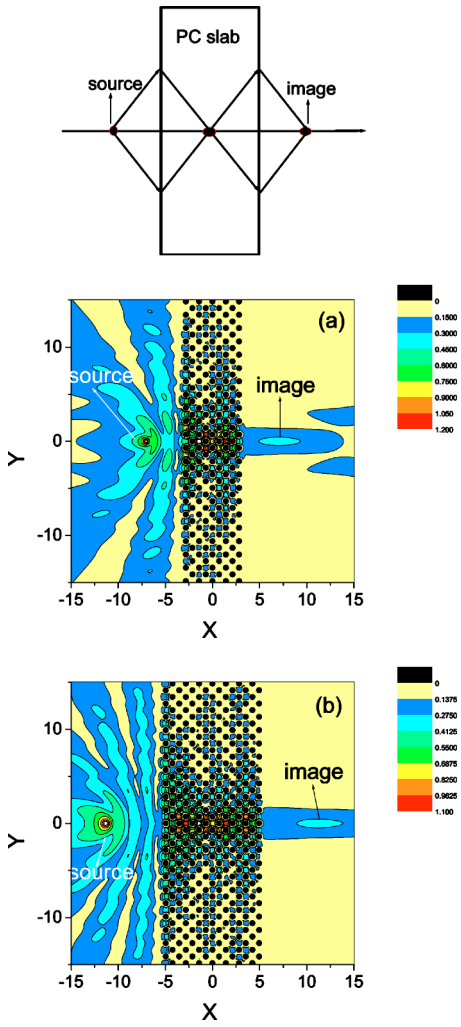

FIG. 4. (a) The intensity distributions of a point source and its image across a $7a$ 2D PC slab at frequency $\omega=0.317(2\pi c/a)$. (b) The corresponding case for a slab with $11a$ thickness. Schematic picture depicting the lensing of a source by a PC slab to an image is shown on top of the figure. The crystal and parameters are identical to those in Fig. 1.

4(b). X and Y represent the vertical and transverse directions of wave propagation, respectively. The field intensity in Fig. 4 is over a $30a\times30a$ region around the center of the sample. The geometry of the PC slab is also displayed for clarity of view. The high quality image in the opposite side of the slab and the focusing in the middle of the slab according to the wave-beam negative refraction law are observed clearly. In order to clarify the sample thickness dependence of the image and focusing, we have also checked a series of slab samples with various thickness. Similar phenomena have also been observed for the thick slabs. For example, Fig. 4(a) shows the calculated field energy pattern for a $7a$ thick sample. A monochromatic line source is placed at a distance of half the thickness of the sample ($3.5a$) from the left surface of the slab and its image is found again near the symmetric position in the opposite side of the slab. A closer look at the data reveals a full transverse size of the central peak

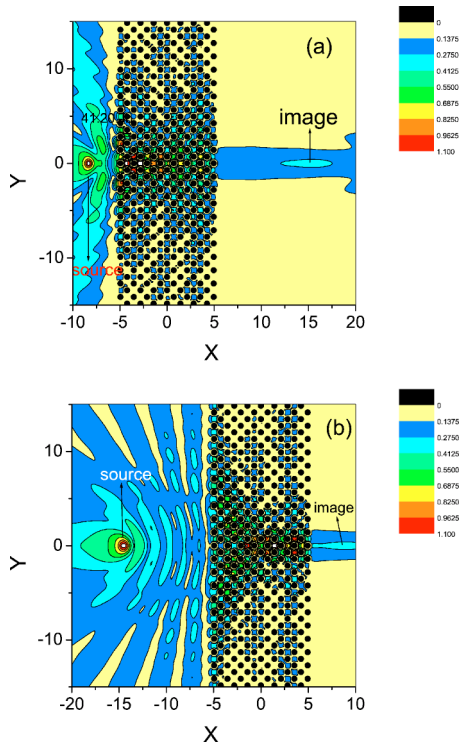

FIG. 5. The intensity distributions of point sources and their images across an $11a$ 2D PC slab at frequency $\omega=0.317(2\pi c/a)$. (a) and (b) represent the cases with different source positions, distances $2a$ and $9a$ from the left surface of the slab, respectively. The crystal and parameters are identical to those in Fig. 1.

about 1.2λ, which is near the conventional diffraction limit. In addition, we find that the transmission efficiencies are 32% and 36% in the presence and absence of the absorption, respectively. The main loss is associated with a finite reflection on the interface of the sample.

To have a more complete vision of the imaging effect of this type of flat lens, we move the light source and see what happens to the imaging behavior. We first put a line source near the left surface of the slab at a $2.0a$ distance from the left surface. The calculated intensity distribution is plotted in Fig. 5(a). The image is found near $9a$ from the right surface. The corresponding result when a line source is far from the left surface is displayed in Fig. 5(b). In this case, the line source is placed at a distance of $9.0a$ from the left surface of the sample and the image is found near $2a$ from the right surface. We test the various positions of the source and image; similar phenomena can be found. These observations indicate clearly that the imaging behaviors depend on the slab thickness and the object distance, following explicitly the well-known wave-beam negative refraction law.

In summary, based on exact multiple-scattering numerical simulations and physical analysis, we have investigated the image behaviors of a 2D metal-dielectric PC with a square lattice by adopting a realistic dielectric constant for the metal components. Subwavelength far-field focusing and imaging, explicitly following the well-known wave-beam negative

refraction law with relative refractive index of −1, have been realized by such a PC structure through choosing suitable scatterers for the lowest valence band.

Note added. Recently, we found that a similar phenomenon in square arrays of silver nanowires was pointed out by Hu and Chan [36].

This work was supported by the National Natural Science Foundation of China (Grant No. 10374009) and the National Key Basic Research Special Foundation of China under Grant No. 2001CB610402. The project was sponsored by SRF for ROCS, SEM, and a Grant from Beijing Normal University.

[1] V. G. Veselago, Sov. Phys. Usp. **10**, 509 (1968).
[2] D. R. Smith, W. J. Padilla, D. C. Vier, S. C. Nemat-Nasser, and S. Schultz, Phys. Rev. Lett. **84**, 4184 (2000).
[3] R. A. Shelby, D. R. Smith, and S. Schultz, Science **292**, 77 (2001).
[4] J. B. Pendry, Phys. Rev. Lett. **85**, 3966 (2000).
[5] P. Markos, I. Rousochatzakis, and C. M. Soukoulis, Phys. Rev. E **66**, 045601(R) (2002).
[6] S. Foteinopoulou, E. N. Economou, and C. M. Soukoulis, Phys. Rev. Lett. **90**, 107402 (2003).
[7] Y. Zhang, B. Fluegel, and A. Mascarenhas, Phys. Rev. Lett. **91**, 157404 (2003).
[8] A. A. Houck, J. B. Brock, and I. L. Chuang, Phys. Rev. Lett. **90**, 137401 (2003).
[9] C. G. Parazzoli, R. B. Greegor, K. Li, B. E. C. Koltenbah, and M. Tanielian, Phys. Rev. Lett. **90**, 107401 (2003).
[10] *Negative Refraction and Metamaterials*, focus issue of Opt. Express **11**, 7 (2003).
[11] G. Shvets, Phys. Rev. B **67**, 035109 (2003).
[12] V. A. Podolskiy, A. K. Sarychev, and V. M. Shalaev, Opt. Express **11**, 735 (2003).
[13] S. A. Ramakrishna and J. B. Pendry, Phys. Rev. B **67**, 201101(R) (2003).
[14] R. Merlin, Appl. Phys. Lett. **84**, 1290 (2004).
[15] L. Chen, S. He, and L. Shen, Phys. Rev. Lett. **92**, 107404 (2004).
[16] D. R. Smith, D. Schurig, J. J. Mock, P. Kolinko, and P. Rye, Appl. Phys. Lett. **84**, 2244 (2004).
[17] Zhaowei Liu, Nicholas Fang, Ta-Jen Yen, and Xiang Zhang, Appl. Phys. Lett. **83**, 5184 (2003).
[18] A. Grbic and G. V. Eleftheriades, Phys. Rev. Lett. **92**, 117403 (2004).
[19] A. N. Lagarkov and V. N. Kissel, Phys. Rev. Lett. **92**, 077401 (2004).
[20] H. Kosaka, T. Kawashima, A. Tomita, M. Notomi, T. Tamamura, T. Sato, and S. Kawakami, Phys. Rev. B **58**, R10096 (1998).
[21] M. Notomi, Phys. Rev. B **62**, 10696 (2000).
[22] B. Gralak, S. Enoch, and G. Tayeb, J. Opt. Soc. Am. A **17**, 1012 (2000).
[23] S. Foteinopoulou and C. M. Soukoulis, Phys. Rev. B **67**, 235107 (2003).
[24] C. Luo, S. G. Johnson, J. D. Joannopoulos, and J. B. Pendry, Phys. Rev. B **65**, 201104R (2002).
[25] E. Cubukcu, K. Aydin, E. Ozbay, S. Foteinopoulou, and C. M. Soukoulis, Nature (London) **423**, 604 (2003).
[26] P. V. Parimi, W. T. Lu, P. Vodo, and S. Sridhar, Nature (London) **426**, 404 (2003).
[27] E. Cubukcu, K. Aydin, E. Ozbay, S. Foteinopoulou, and C. M. Soukoulis, Phys. Rev. Lett. **91**, 207401 (2003).
[28] P. V. Parimi, W. T. Lu, P. Vodo, J. Sokoloff, J. S. Derov, and S. Sridhar, Phys. Rev. Lett. **92**, 127401 (2004).
[29] A. Berrier, M. Mulot, M. Swillo, M. Qiu, L. Thylen, A. Talneau, and S. Anand, Phys. Rev. Lett. **93**, 073902 (2004).
[30] C. Luo, S. G. Johnson, J. D. Joannopoulos, and J. B. Pendry, Phys. Rev. B **68**, 045115 (2003).
[31] Z. Y. Li and L. L. Lin, Phys. Rev. B **68**, 245110 (2003); C. H. Kuo and Z. Ye, Phys. Rev. E **70**, 026608 (2004).
[32] X. Zhang, Phys. Rev. B **70**, 205102 (2004).
[33] X. Zhang, Phys. Rev. B **70**, 195110 (2004).
[34] X. Wang, Z. F. Ren, and K. Kempa, Opt. Express **12**, 2919 (2004).
[35] L. M. Li, Z. Q. Zhang, and X. Zhang, Phys. Rev. B **58**, 15589 (1998); M. M. Sigalas, C. T. Chan, K. M. Ho, and C. M. Soukoulis, *ibid.* **52**, 11744 (1995).
[36] X. Hu and C. T. Chan, Appl. Phys. Lett. **85**, 1520 (2004).